Temperature Dependence of the Zero-Field Splitting Parameter D of Cr^{3+} Ions in $CsAl(SO_4)_2 \cdot 12H_2O$

Gerald B. Stevenson

A THESIS

in

The Department

of

Physics

Presented in Partial Fulfillment of the Requirements for the Degree of Master of Science at

Sir George Williams University

Montreal, Canada

April, 1974

Abstract

Temperature Dependence of the Zero-Field Splitting Parameter D of Cr^{3+} Ions in $CsAl(SO_4)_2 \cdot 12H_2O$

Gerald B. Stevenson

In this particular study a crystal of caesium aluminum sulfate dodecahydrate ($CsAl(SO_4)_2 \cdot 12H_2O$), or more commonly referred to as caesium aluminum alum was doped with Cr^{3+} and examined with a Varian X-band microwave (Electron Paramagnetic Resonance) spectrometer.

Absorption spectra were obtained at various temperatures and from this data the zero magnetic field splitting parameter, D, of the paramagnetic Cr^{3+} ions was calculated as a function of temperature.

A spin Hamiltonian approach with $S = 3/2$ and $g = 1.975 \pm 0.005$ was used to describe the spectrum.

The value of D varied from -0.074 ± 0.0003 cm^{-1} at room temperature (290 °K) to -0.070 ± 0.0003 cm^{-1} at 4.2 °K.

Table of Contents

Table of Contents cont.

Acknowledgement

The author wishes to thank Dr. J. A. MacKinnon for his constant assistance and encouragement throughout the course of this research; particularly in the latter stages when we were literally cities apart.

The use of McMaster University library facilities and Westinghouse Canada office facilities were greatly appreciated during the final stages of this thesis.

Introduction

a) Alums.

From the onset of Electron Paramagnetic Resonance (EPR) research, the alum family has played a significant role. After the first observation of EPR by E. Zaviosky[1], the experimental work in the field concentrated on the alums and Tutton salts that contained transitions ions in their normal composition. In this instance, a transition ion is imbedded within a diamagnetic host alum.

The alums have proven to be convenient hosts since most of the paramagnetic elements can be readily substituted as impurities in them. Those alums that are paramagnetic by nature (eg. $KCr(SO_4)_2 \cdot 12H_2O$) were studied by many authors including Baggley and Griffiths (1947) and Kip et al (1951). The latter paper included studies of various chrome alums and presented zero field splitting measurements as a function of temperature. They found $g = 1.98$ and $D = -0.067\ cm^{-1}$ for CsCr alum, very close to the values determined in this paper.

The crystal structure of the alums was determined by Lipson (1935) and Lipson and Beevers (1935). Their conclusions provided the groundwork for later EPR interpretations of alum-hosted ions (since it is necessary to have accurate atomic dimensions for the compound being studied in order to apply perturbation theory and determine the crystalline fields acting on the paramagnetic ion).

[1] E.J. Zavoisky, J. Phys. USSR 9, 211 (1945).

b) Paramagnetism and EPR Concepts

At this point some mention of the significance of paramagnetism and some of the characteristics of paramagnetic substances will be made. This will be treated in greater detail in Chapter 2. Paramagnetic substances have unpaired electronic spins and this results in degenerate spin states. Expanding on this, paramagnetic substances can be typified as having an odd number of electrons, partly filled inner shells or compounds having resultant angular momenta.

In EPR studies an external magnetic field is applied to the paramagnetic sample thus removing some of the degeneracy by ensuring the spins are ordered either parallel or anti-parallel to the field. Transitions between the resulting non-degenerate energy levels are then induced by an incident microwave field which is perpendicular to the external magnetic field. The resonance condition is met when the relationship $h\nu = g\beta H$ is satisfied. Here, h is Planck's constant, ν is the microwave frequency, g is the spectroscopic splitting factor, β is the Bohr magneton and H is the value of the magnetic field.

c) Cr^{3+}

The free ion Cr^{3+} has a $^4F_{3/2}$ ground state, that is, the orbital degeneracy (2L+1) is 7 and spin degeneracy (2S+1) is 4. In the case of the compound under study,

the imbedded ion is surrounded by six water molecules as nearest neighbors. These molecules create an axially symmetric electrostatic field around the Cr^{3+} ion and reduce the degeneracy as shown in figure 4. The electric field felt by the paramagnetic ion has been calculated by Kleiner (1952) and Freeman and Watson (1960).

Cr^{3+} has been extensively studied in various environments for EPR. The 3d shell has 3 electrons and is in the transition group. Particular emphasis has been in connection with the ruby laser (Al_2O_3).

d) Temperature and EPR

Electron paramagnetic resonance studies tend to be conducted at three "benchmark" temperatures depending on the temperature range that resonance appears. The primary temperatures include room temperature ($\sim$ 290 °K), the boiling point of Nitrogen (77 °K) and that of Helium (4.2 °K). In this paper, the range from 300 °K to 4.2 °K was examined. Sufficient intermediate temperatures were used to adequately define the zero-field splitting factor D over this range.

The stable temperature range of the standard Varian V-4502 spectrometer was extended beyond the three "bench-mark" temperatures referred to above, by variable temperature apparatus constructed by MacKinnon (1972).

e) Significance of EPR

The experimental techniques of EPR are sufficiently refined to provide accuracy to within ± 0.0005 % when using this method to determine energy level splittings. This was the principle use of EPR and remains as the outstanding achievement in this area of spectroscopy.

Other important data readily available from EPR spectra include the interactions betweens electrons and the lattice (affects the line width of absorption) as well as the interactions due to nuclear magnetic moments (hyperfine structure). As the measure of D ultimately defines the energy level structure of paramagnetic compounds in a particular sample, the determination of this parameter is of considerable interest in the total description of Cr^{3+}. (See figures 4 and 8.)

Chapter 1

Crystallography

The crystal growth technique for the $CsAl(SO_4)_2 \cdot 12H_2O$ crystal was documented by MacKinnon (1968). In this technique a saturated solution of aluminum sulphate, caesium sulphate and a small amount of chromium sulphate is allowed to cool. Because of the pronounced symmetry in the crystal morphology, the sample can be readily oriented in specific planes. In this study the sample was oriented with the $\{111\}$ plane parallel to the external magnetic field of the spectrometer.

The basic alums are double salts with the formulae:

$$R^{1+}R^{3+}(R^{6+}O_4)_2 \cdot 12H_2O$$

according to Lipson (1935) and Lipson and Beevers (1935). The R^{1+} can be one of the following: Na, K, NH_4, Rb, Cs, or Tl. The R^{3+} can be Al, Cr, Fe, Ga, V, or Ir. R^{6+} is usually S but can also be Se or Te.[2]

The alum family is further categorized into α, β, and γ types. These are determined by the physical size of the R^n and were labelled by Lipson (1935). He found that the size of the monovalent ion is most significant

[2] Mellor, J.W., A Comprehensive Treatise on Inorganic and Theoretical Chemsitry, Vol. V, p. 341, Longmans, Green and Company, London, 1924; as quoted by G.F. Dionne (1964)

in determining the category of alum. (These alum types are further elaborated on by Jona and Shirane (1962).)

The β alums are characterized by large monovalent ions; the γ type has small monovalent ions and the α type makes up the majority with intermediate monovalent ions.

CsAl alum is a β type and is characterized by the SO_4 complex getting closer to the Cs ion. The β type are often thought of as "distorted" α type alums as the SO_4 is forced to take up a new position due to the different atomic diameters of the ions involved. (The atomic radii for the ions of interest are as follows: Cs 1.67 Å; Cr^{3+} 0.63 Å; and Al^{3+} 0.51 Å.)[3]

There are four molecules per unit cell for CsAl alum and these are arranged as depicted by the 1/8 unit cell in figure 5. Recent neutron diffraction measurements by Cromer et al (1966) provided more accuracy than Lipson (1935) but really only confirmed the earlier configurations.

As previously mentioned, the Cr^{3+} (or the Al^{3+}) are surrounded by the octahedron of water molecules as nearest neighbors and this is another property β alums. The secondary and other neighbors have minimal effects on the paramagnetic Cr^{3+}.

[3] Handbook of Chemistry and Physics, p. 3507, 44th ed.

The Cr^{3+} ion is physically displacing a certain amount of Al^{3+} in the chemical process for the compound studied. The small percentage of Cr^{3+} (0.18%) is attributed to the very localized absorption of the foreign ion.

From elementary chemical relationships, if the alum was $CsCr(SO_4)_2 \cdot 12H_2O$, the chromium content would be 8.77% by weight.

Chapter 2

EPR Theory

a) Magnetic Moments

The magnetic moment $\vec{\mu}$ associated with a free electron and influenced by a steady magnetic field will tend to align itself to the field $\vec{H}$ according to the energy relationship $E = - \vec{\mu} \cdot \vec{H}$.

In the case of paramagnetic substances the unpaired electron spins have the same tendency but to a different degree. In this case the overall magnetic moment of the sample is related to the angular momentum by

$$\vec{\mu} = g\beta\vec{J}$$

where g is the spectroscopic splitting factor and the Bohr magneton

$$\beta = \frac{ge\hbar}{2m}$$

The total angular momentum operator $\vec{J}$ is made up of the angular momentum $\vec{L}$ and the spin angular momentum $\vec{S}$ operators. (For Russel-Saunders coupling $\vec{J} = \vec{L} + \vec{S}$.) Magnetic resonance occurs when transitions between the $2J + 1$ energy levels occur.

b) Paramagnetism

An essential difference between diamagnetic and paramagnetic substances can be described by the sign of

the susceptibility χ. The permeability u and the susceptibility χ are defined by the relation $\vec{B} = u\vec{H} = u_o \cdot (\vec{H} + \vec{M}) = u_o \vec{H}(1 + \chi)$ where $\vec{M}$ is the magnetization (magnetic moment per unit volume). Diamagnetic substances have a positive susceptibility.

c) Spin Hamiltonian

After Abragam and Pryce's (1951) original work on the Spin Hamiltonian concept to relate experimental observations to a phantom Hamiltonian, the theoretical aspect of EPR was more manageable and the experimental results were reported in a manner readily adaptable to the Spin Hamiltonian concept.

As described precisely by Poole (1967) and others, the Spin Hamiltonian is represented as follows:

$$H_S = H_{Coulomb} + H_{Crystal\ Field} + H_{Spin\text{-}Orbit} + H_{Spin\text{-}Spin} + H_{Zeeman} + H_{Hyperfine} + H_{Quadrupole} + H_{Nuclear}$$

EPR studies are concerned primarily with the Zeeman interaction. For a free ion, this affects the energy levels W (say of the free electron) by the relation

$$W = g\ \beta\ H\ M$$

where the resultant angular momentum J is acted on by a magnetic field H. M is the component of angular momentum J parallel to the external field, g is the Lande g factor

given by

$$g = 1 + \frac{J(J + 1) + S(S + 1) - L(L + 1)}{2J(J + 1)}$$

and L and S are orbital and spin components as previously noted.

The external magnetic field of the spectrometer separates the degenerate spin states. If the spin is parallel to the field the quantum number denoted m_s is equal to +1/2, the magnetic moment equals $1/2\ g\ u_B$ and the energy is $-\ 1/2\ g\ u_B\ H$. The signs are opposite for the antiparallel case.

The Spin Hamiltonian concept is related to the EPR phenomena of the flip-flop process of the angular momenta of the electrons in the multi-electron case by treating the various interactions involved as perturbations.

d) Crystal Field

One must consider the interactions of the surrounding ions and molecules and how they affect the Cr^{3+} ion in this case. The point-charge or crystal field model has been used as an intermediate approach to picture this situation. In the region of the paramagnetic Cr^{3+} ion it is assumed the charge density arises from this ion alone and the density is spherically symmetric.

The potential from the host lattice is assumed

not to penetrate the region and satisfies LaPlace's equation. That is, this is an isolated spin system interacting with an external symmetric crystal and field.

Unfortunately this elementary approach does not hold for the iron group as the d wave functions overlap the wave functions of the neighboring (H_2O) ligands (per Low (1960)). The wave functions of the complexes cannot be divorced.

However, because of the axially symmetric nature of the perturbing field (ie the neighboring six H_2O molecules lie in a regular octahedron around the Cr^{3+} ion), the system can be described in Spin Hamiltonian format as follows

$$H = \beta\{g_{||} H_z S_z + g_{\perp} (H_x S_x + H_y S_y)\}$$

$$+ D\{S_z^2 - 1/3\, S(S+1)\}$$

where the term in D corresponds to the second order crystal field effects on the energy levels in zero magnetic field. That is, it includes the spin-orbit and spin-spin interactions. β is the Bohr magneton and the nuclear (lower order effects--if present) have been omitted.

e) Resonance condition

Bleaney (1951) derived the following formula for the anisotropic case being considered. The angle θ takes into account the effect of the external magnetic field when it is at an angle θ with respect to the true crystalline field of the compound.

$$h\nu = gBH + D(M - 1/2)\left\{\beta \frac{g_{\parallel}^2}{g^2}\cos^2\theta - 1\right\}$$
$$- \left(\frac{Dg_{\parallel}\, g_{\perp}\cos\theta\sin\theta}{g^2}\right)^2 \frac{1}{2g\beta H_o}\{4S(S+1)-24M(M-1)-9\}$$
$$+ \left(\frac{Dg_{\perp}^2\sin^2\theta}{g^2}\right)^2 \frac{1}{8g\beta H_o}\{2S(S+1)-6M(M-1)-3\}$$

H is the magnetic field for resonance, $H_o = \frac{h\nu}{gB}$, ν is the microwave frequency, g is the spectroscopic splitting factor and $g^2 = g_{\parallel}^2\cos^2\theta + g_{\perp}^2\sin^2\theta$.

It should be noted that for $\theta = 0$ the magnetic field is parallel to the crystalline axis and the second order terms (D^2) are zero. This implies the energy levels are equally separated in the magnetic field and D can thus be determined directly.

If the incident microwave radiation (wavelength^{-1}) is less than the zero-field splitting parameter, there would not be observable resonance. This was not the case for the Cr^{3+} situation (D is of the order of $|0.07|$ cm^{-1} and the incident radiation is of the order of 0.3 cm^{-1}).

Chapter 3

Significance and Determination of D

With reference to figure 4, the Cr^{3+} ion is split into two Kramer's doublets after the cubic and axial fields from the surrounding complexes reduce the orbital degeneracy. These doublets are separated by a measurable quantity D in energy terms cm^{-1}.

For dilute compounds where the spin-spin and exchange interaction is negligible, D is approximately zero. Because of the large separation of secondary field influences for the Cr^{3+} in CsAl alum, the quantity D is quite small.

The most obvious spectrometer for determining the zero-field splitting parameter would of course be a variable frequency spectrometer where the magnetic field could be set to zero and the frequency changed to determine the resonance characteristics. In this case, the splitting parameter D could be obtained with little manipulation.

The use of a fixed frequency spectrometer and extrapolating the zero-field case from the higher field cases is the normal method of measurement however, since fixed frequency spectrometers are most practical for other EPR work and found in most laboratories.

Chapter 4

Experimental Apparatus

A commercially available Varian V-4502 spectrometer equipped with a V-4500-42 X-band microwave bridge and V-K3525 superhetrodyne accessory was used in this experiment. The variable temperature apparatus was integrated in the Varian subassembly as described by MacKinnon (1972). Essentially, the heating element is a wire wrapped around the resonant cavity and connected to a power supply. The applied power regulates the temperature.

A platinum resistance thermometer was used (Rosemount Engineering model 137AA). A constant current source was fed through the thermometer (approximately 1μa current) and the temperature was read as a function of voltage which was in turn a measure of the resistance of the thermometer.

With reference to the schematic (figure 6), the basic components of a variable magnetic field EPR spectrometer will be briefly described.

The paramagnetic sample is situated in a resonant microwave cavity (rectangular TE_{102} mode). The klystron irradiates the sample at a frequency ν adjustable between 8.8 and 9.6 Ghz. This field is perpendicular to the dc magnetic field H. The magnetic field is continuously

adjustable from 1 gauss to 10 kilogauss. In the normal sweep mode this magnetic field varies linearly with time.

The klystron energy is coupled via an isolator, attenuator and magic tee. The latter component is balanced at one temperature and must be rebalanced as the cavity temperature is varied. The sample cavity is connected to one part of the magic tee, a second klystron is connected to another port and a detector assembly is on the remaining port.

The reflected microwave power from the sample cavity is demodulated in the combiner/detector area of the magic tee. The intermediate (30 Mhz) frequency is then amplified and fed into a second demodulator together with the magnetic field modulation frequency. After several stages of trimming the output derivative of the ESR signal is recorded on a chart recorder.

The main dewar assembly is held stationary and the magnet is rotated as required about the sample. The inner and outer dewars contain liquid helium and nitrogen respectively for low temperature applications.

A standard Varian NMR flux meter was used for magnetic field measurements. Measurement of the incident microwave frequency was determined using the DPPH (diphenyl picryl hydrazl) standard which was affixed at the bottom of the resonant cavity.

Chapter 5

Experimental Procedure

The magnetic field was calibrated with an NMR probe as mentioned. The probe is positioned in the center of the magnetic field and is connected to a frequency counter. The relationship $H = 0.2349\ f$ was used for the proton probe used. The constant varies with the probe type. The thermometer was calibrated by the supplier.

The sample was oriented in the desired plane at the base of the microwave cavity along with a trace of DPPH. Since the linewidth of DPPH is two to three gauss and its resonance is very pronounced, it serves as the most suitable reference for this work.

From this point on, it is necessary to lower the temperature of the sample in two steps. First, the outer dewar is filled with liquid nitrogen to reduce its temperature to 77 °K. This surrounds the inner dewar which in turn surrounds the cavity and sample. The inner dewar is loaded with liquid helium and the temperature is reduced to 4.2 °K. The two dewars are separated by a vacuum and this, coupled with the low temperature of the outer dewar, tend to shield the lower chamber and reduce heat loss and incident "warm" radiation.

Once the temperature is stabilized at a particular temperature and the klystron-related adjustments made, a sweep from 1 to 5000 gauss is conducted at an angle θ.

The frequency is measured with a wavelength meter (for comparison purposes) and the chart recording tabulated with temperature and magnetic field values.

For each temperature the magnet angle (with reference to the crystallographic axes) was varied at 5° intervals from 0° to ±90°.

The derivative measurements on the chart recordings are the obvious peaks on the attached sample trace (Figure 11). Theoretically, when there is no resonance the graph should be a horizontal trace. Deviations from the horizontal situation are some measure of the noise of the system. However, this does not obscure the prominent resonant signals.

Once the run was finished for a particular temperature, the temperature was changed and stabilized; the results were then obtained for a new temperature.

Chapter 6

Experimental Results

The various plots of θ (orientation of the magnetic field with relation to the crystalline field) versus the magnetic field strength was graphed for future reference and to confirm the crystal orientations. The spectrum has twelve lines, three from each of the four equivalent magnetic complexes per unit cell (refer to figure 7).

The field values of the "horizontal" traces were determined and substituted in equation (A.11) to obtain the value of D.

The temperature of the sample was determined from the resistance/voltage measurements as outlined previously. This is tabulated in table 1 below:

Table 1 (Refer to Fig. 9)

Resistance (ohms)	Temperature (°K)
1512	298
1250	244
1000	205
680	150
254.8	76
180	66
5.1	4.2

The value of g and D was derived from equations (A.10) and (A.11) and those results are tabulated in table 2 below. The values of H_1 and H_2 are the fields of the horizontal traces.

Table 2

Temp (°K)	H_1 (gauss)	H_2 (gauss)	H_{DPPH} (gauss)	g	D (cm^{-1})
4.2	2674.9	4204.2	3391.9	1.9764	-0.07049
66.0	2679.4	4208.5	3383.3	1.9688	-0.07029
76.0	2680.3	4204.8	3395.9	1.9765	-0.07035
150.0	2861.4	4213.0	3397.6	1.9797	-0.07157
205.0	2659.7	4222.1	3396.0	1.9733	-0.07207
244.0	2645.8	4226.1	3393.4	1.9788	-0.0730
298.0	2633.6	4246.9	3384.9	1.9719	-0.07426

The energy level diagram of Cr^{3+} in an axial field is illustrated in figure 4 and as previously noted, the cubic electric field splits the ^4F ground state into a low lying singlet (designated Γ_2) and the two higher lying triplets (designated Γ_5 and Γ_4 according to standard nomenclature).

The axial crystal field further splits the electronic singlet (with spin degeneracy) into two Kramer's doublets separated by the amount D as shown above. This is illustrated in figure 10.

Chapter 7

Summary and Discussion

a) General

The zero-field splitting parameter D was determined as outlined in the previous chapter with the aid of a variable field, fixed frequency EPR spectrometer. Although the use of a variable frequency klystron would have provided a more straightforward approach, the present case was greatly simplified because of the existence of Bleaney's (1951) work. Also, a klystron with a frequency range over three orders of magnitude is neither manufactured nor is it too practical for the average laboratory to have three klystrons over the necessary ranges to provide direct calculations for the zero magnetic field case.

b) Errors

The accuracy of the temperature and the zero-field splitting factor are a function of several parameters. These are outlined in relative order of magnitude:

1) The temperature calibration and reading results in an error of ± .2 °K.
2) The magnetic field is accurate to ± 0.05%.
3) The klystron frequency is accurate to 1 in 10^6.
4) The values of β and h are assumed to be accurate to .001%.

Noise sources and their effects as well as the chart recorder response were weighted in the above. The background noise only affected the plots on the "rise" or "fall" of the recordings and since these were averaged out, minimal error is expected from reading the traces. Feher (1957) has excellent notes regarding the sensitivity and the mechanical factors relating to the overall error performance of a spectrometer.

c) Conclusions

The variation of D with temperature and indeed even the D factor at a fixed temperature is a function of different factors, depending on the environment of the particular sample. In this case it is assumed the triplet state (the lowest one) is the source of most orbital coupling and the parameter D is a somewhat removed measure of this effect.

Although these values correspond very closely to Kip et al (1951) calculations of g = 1.98 and D = -0.067 cm^{-1} results for $CsCr(SO_4)_2 \cdot 12H_2O$, it may be of interest to determine how the ratio of Cr^{3+} in CsAl alum affects the zero field splitting factor. It is expected that this would not alter D appreciably because large-scale distortions are not likely to occur as the Cr and Al radii are relatively close and they are of course both trivalent.

Appendix

The following formula is due to Bleaney (1951):

$$h\nu = g\beta H + D(M-1/2)\left\{\frac{3g_{\parallel}^2}{g^2}\cos^2\theta - 1\right\} \qquad (A.1)$$

$$- \left(\frac{Dg_{\parallel}\, g_{\perp}\cos\theta\sin\theta}{g^2}\right)^2 \frac{1}{2g\beta H_o}\left\{4S(S+1) - 24M(M-1) - 9\right\}$$

$$+ \left(\frac{Dg_{\perp}^2 \sin^2\theta}{g^2}\right)^2 \frac{1}{8g\beta H_o}\left\{2S(S+1) - 6M(M-1) - 3\right\}$$

where H is the magnetic field for resonance, $H_o = \frac{h\nu}{gB}$, ν is the microwave frequency, g is the spectroscopic splitting factor and $g^2 = g_{\parallel}^2\cos^2\theta + g_{\perp}^2\sin^2\theta$.

Assuming that g is isotropic, ie. $g_{\parallel} = g_{\perp} = g$, then

$$h\nu = g\beta H + D(M-1/2)\left\{3\cos^2\theta - 1\right\} \qquad (A.2)$$

$$- (D\cos\theta\sin\theta)^2 \frac{1}{2g\beta H_o}\left\{4S(S+1) - 24M(M-1) - 9\right\}$$

$$+ (D\sin^2\theta)^2 \frac{1}{8g\beta H_o}\left\{2S(S+1) - 6M(M-1) - 3\right\}$$

Solving for H and letting $P = 4S(S+1) - 24M(M-1) - 9$

$$Q = 2S(S+1) - 6M(M-1) - 3 \qquad (A.3)$$

$$R = M - 1/2$$

leads to $H = \frac{h\nu}{g\beta} - \frac{DR}{g\beta}\left\{3\cos^2\theta - 1\right\} + D^2\cos^2\theta\sin^2\theta\frac{P}{2g^2\beta^2 H_o}$

$$- D^2\sin^4\theta\frac{Q}{8g^2\beta^2 H_o} \qquad (A.4)$$

Recalling the identities $\sin^2\theta = 1 - \cos^2\theta$ and

$$\sin^4\theta = (1-\cos^2\theta)^2 = 1 - 2\cos^2\theta + \cos^4\theta \qquad \text{(A.5)}$$

then
$$H = \frac{h\nu}{g\beta} + \frac{DR\ 3\cos^4\theta}{g\beta} + \frac{DR}{g\beta} \qquad \text{(A.6)}$$

$$+ D^2\cos^2\theta\ (1-\cos^2\theta)\ \frac{P}{2g^2\beta^2H_o}$$

$$- D^2(1-2\cos^2\theta + \cos^y\theta)\ \frac{Q}{8g^2\beta^2H_o}$$

$$= \left(\frac{h\nu}{g\beta} + \frac{DR}{g\beta} - \frac{D^2Q}{8g^2\beta^2H_o}\right) \qquad \text{(A.7)}$$

$$+ \cos^2\theta\ \left(\frac{-3DR}{g\beta} + \frac{D^2P}{2g^2\beta^2H_o} + \frac{2D^2Q}{8g^2\beta^2H_o}\right)$$

$$+ \cos^4\theta\ \left(\frac{-D^2P}{2g^2\beta^2H_o} - \frac{D^2Q}{8g^2\beta^2H_o}\right)$$

The transitions of interest are 1/2 to 3/2 where S = 3/2, M = +3/2. This leads to P = +12, Q = 0 and R = +1. Substituting these values in (A.7) gives:

$$H = \frac{h\nu}{g\beta} + \frac{D}{g\beta} + \cos^2\theta\ \left(\frac{-3D}{g\beta} + \frac{12D^2}{2g^2\beta^2H_o}\right) + \frac{\cos^4\theta(-)12D^2}{2g^2\beta^2H_o} \qquad \text{(A.8)}$$

At resonance the normal assignments shown in figure 7 are used and $\theta = 90°$ so the $\cos\theta$ terms vanish. This leads to

$$H_{RES} = \frac{h\nu}{g\beta} + \frac{D}{g\beta} \qquad \text{(A.9)}$$

The term $\frac{h\nu}{\beta}$ can be replaced by the term gH_o and using the value 2.0037 for g, and the case for the -1/2 to -3/2 transition, $H_{RES} = \frac{h\nu}{g\beta} - \frac{D}{g\beta}$, the simple relationship

$$g = \frac{2g_{DPPH}\ H_{DPPH}}{H_1 + H_2} \qquad (A.10)$$

is arrived at. By a like process the D factor is

$$D = (g\ H_1 - g_{DPPH}\ H_{DPPH})\beta \qquad (A.11)$$

In the above formulae (A.10 and A.11), g relates to Cr^{3+}, g_{DPPH} and H_{DPPH} refer to the frequency of the radiation which is defined by the DPPH values. The fields H_1 and H_2 correspond to the "horizontal" plots shown in figure 7.

Bibliography

References Cited

Abragam, A. and Pryce, M.H.L. Proc. Roy. Soc., A205, 135, 1951.

Bagguley, D.M.S. and Griffiths, J.H.E., Nature 160, 532, 1947.

Bleaney, B. Phil. Mag. 42, 441, 1951.

Cromer, D.T., Kay, M.I. and Larson, A.C. Acta Cryst. 21, 383, 1966.

Feher, G. The Bell System Technical Journal. 449, 1957.

Freeman, A.J. and Watson, R.E. Phys. Rev. 20, 1254, 1960.

Jona, F. and Shirane, G. Ferroelectric Crystals. International Series of Monographs on Solid State Physics. Vol I, 335. Pergamon Press, Oxford, 1962.

Kip, A.F., Davis, C.F., Jennings, L. and Reiner, D. Nuovo Cimento. 8, 683. 1951.

Kleiner, W.H., J. Chem. Phys. 20, 1784, 1952.

Lipson, H. Proc. Roy. Soc. A151, 347, 1935.

Lipson, H. and Beevers, C.A. Proc. Roy. Soc, A148, 664, 1935.

Low, W. Paramagnetic Resonance in Solids. Academic Press, New York, 1960.

MacKinnon, J.A. Rev. Sci. Instrum. 43, 1847, 1972.

MacKinnon, J.A. and Dionne, G.F. Phys. Rev. 172, 325, 1968.

Poole, C.P., Electron Spin Resonance. Interscience Publishers, New York, 1967.

References Consulted

Abragam, A. and Bleaney, B. Electron Paramagnetic Resonance

of Transition Ions. Clarendon Press, Oxford.1970.

Alger, R.S. Electron Paramagnetic Resonance: Techniques and Applications. Interscience Publishers, New York, 1968.

Azaroff, L.V. Introduction to Solids. McGraw Hill, New York, 1960.

Ballhausen, C.J. Introduction to Liquid Field Theory. McGraw Hill, New York, 1962.

Bersohn, M. and Baird, J.C. An Introduction to Electron Paramagnetic Resonance. W.A. Benjamin Inc., New York, 1966.

Bickerton, J.L. M.Sc. Thesis (Unpublished), Sir George Williams University, Montreal 1969.

Dionne, G.F. Ph.D. Thesis (Unpublished), McGill University, Montreal, 1964.

Gordy, W., Smith, W.V. and Tram Barulo, R.F. Microwave Spectroscopy. John Wiley and Sons, New York, 1953.

Ingram, D.J.E. Spectroscopy at Radio and Microwave Frequencies. Plenum Press, New York, 1967.

MacKinnon, J.A. Ph.D. Thesis (Unpublished), McGill University, Montreal, 1968.

MacKinnon, J.A. and Dionne, G.F. Can. J. Phys. 44, 2329, 1966.

Manoogian, A. and MacKinnon, J.A. Can. J. Phys. 45, 2769, 1967.

Orton, J.W. Electron Paramagnetic Resonance; An Introduction to Transition Group Ions in Crystals. Pitman Press, London, 1968.

Pake, G.E. Paramagnetic Resonance. W.A. Benjamin Inc., New York 1962.

Vanier, J. Ph.D. Thesis (Unpublished), McGill University, Montreal, 1962.

Van Vleck, J.H. J. Chem. Phys. 7, 61, 1939.

Wertheim, G.K., Hausman, A. and Sander, W. The Electronic Structure of Point Defects. North-Holland Publishing Co., Amsterdam, 1971.

Whiffen, D.H. Spectroscopy. John Wiley and Sons, New York, 1971.

Woonton, G.A. and MacKinnon, J.A., Can. J. Phys. 46, 59, 1967.

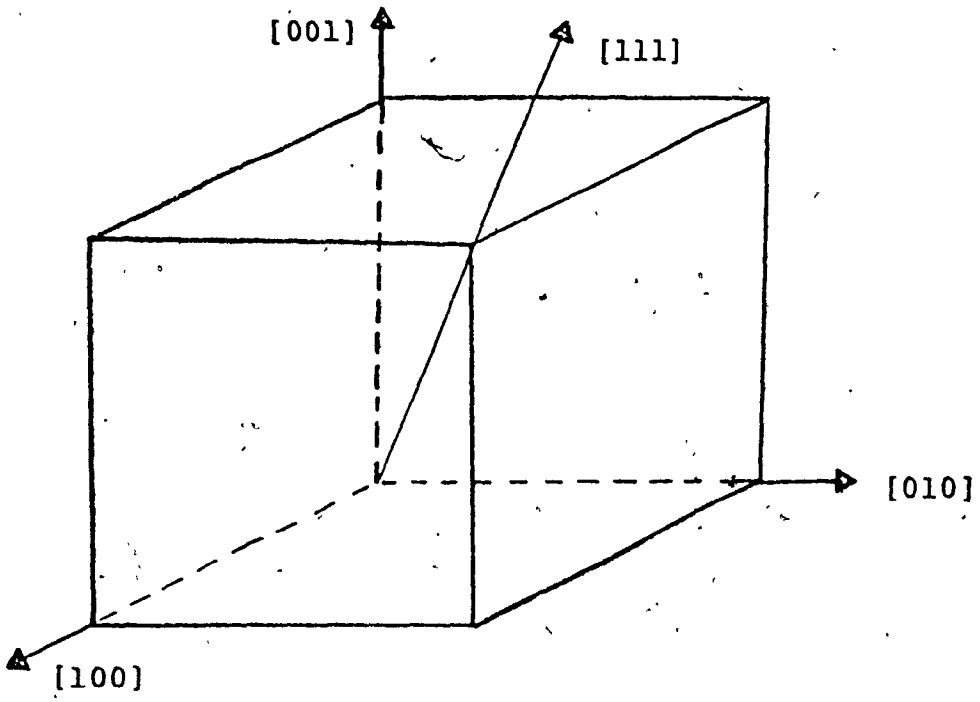

Figure 1. Principle Crystallographic directions.

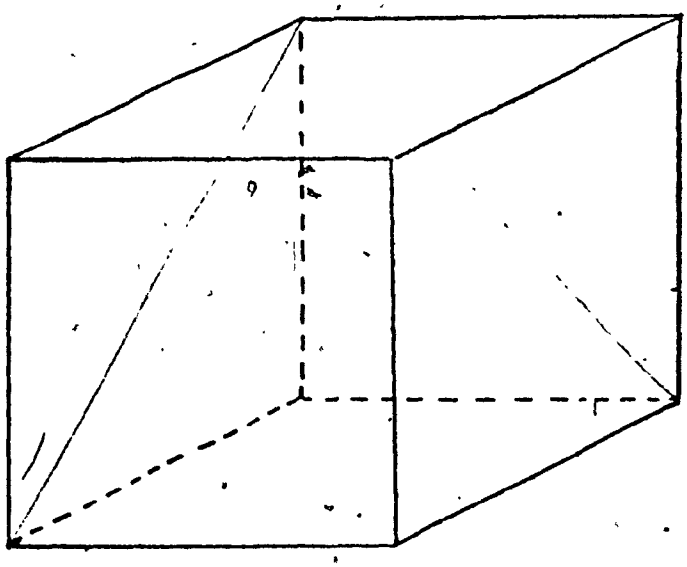

Figure 2. The {111} plane (shaded).

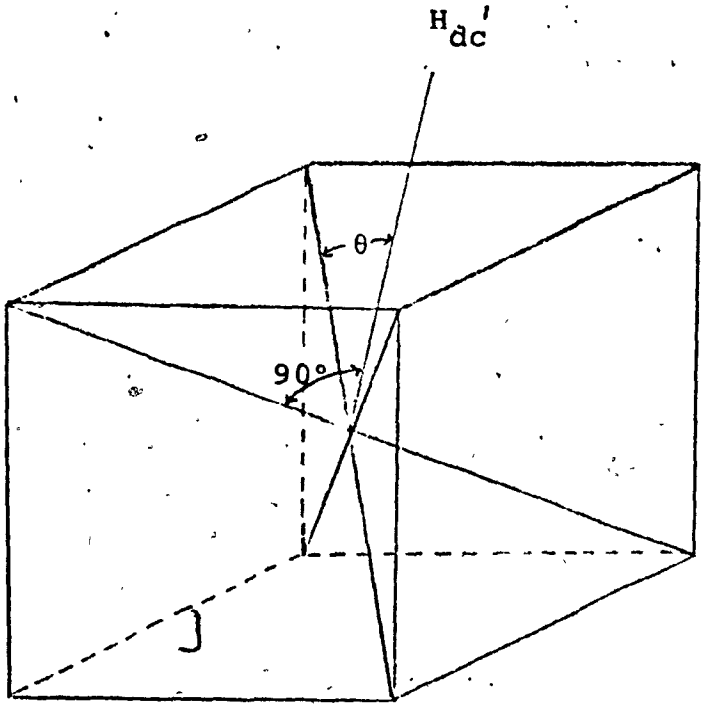

Figure 3. H_{dc} moving in {111} plane.

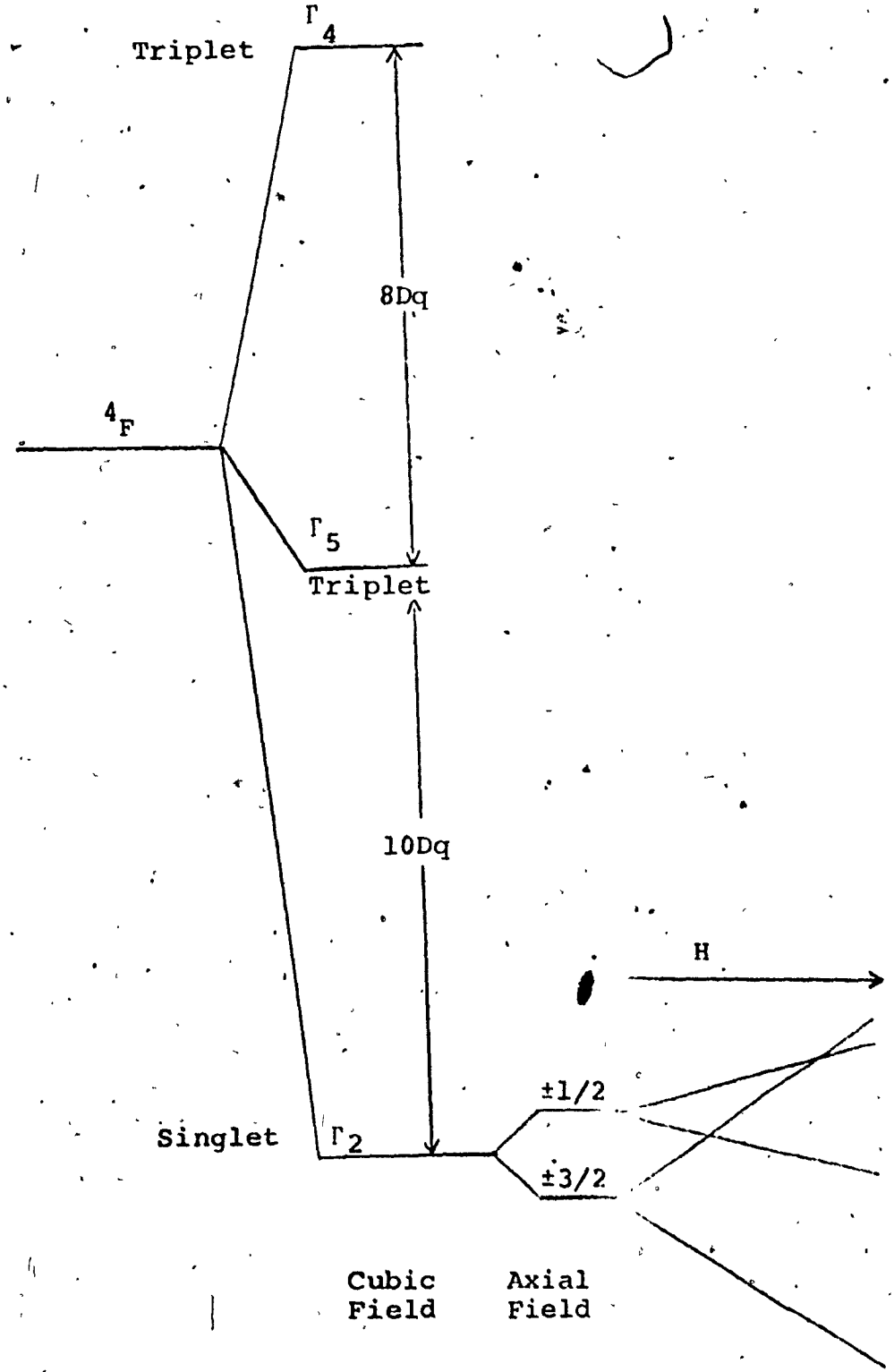

Figure 4. Energy level diagram of Cr^{3+} including external magnetic field H.

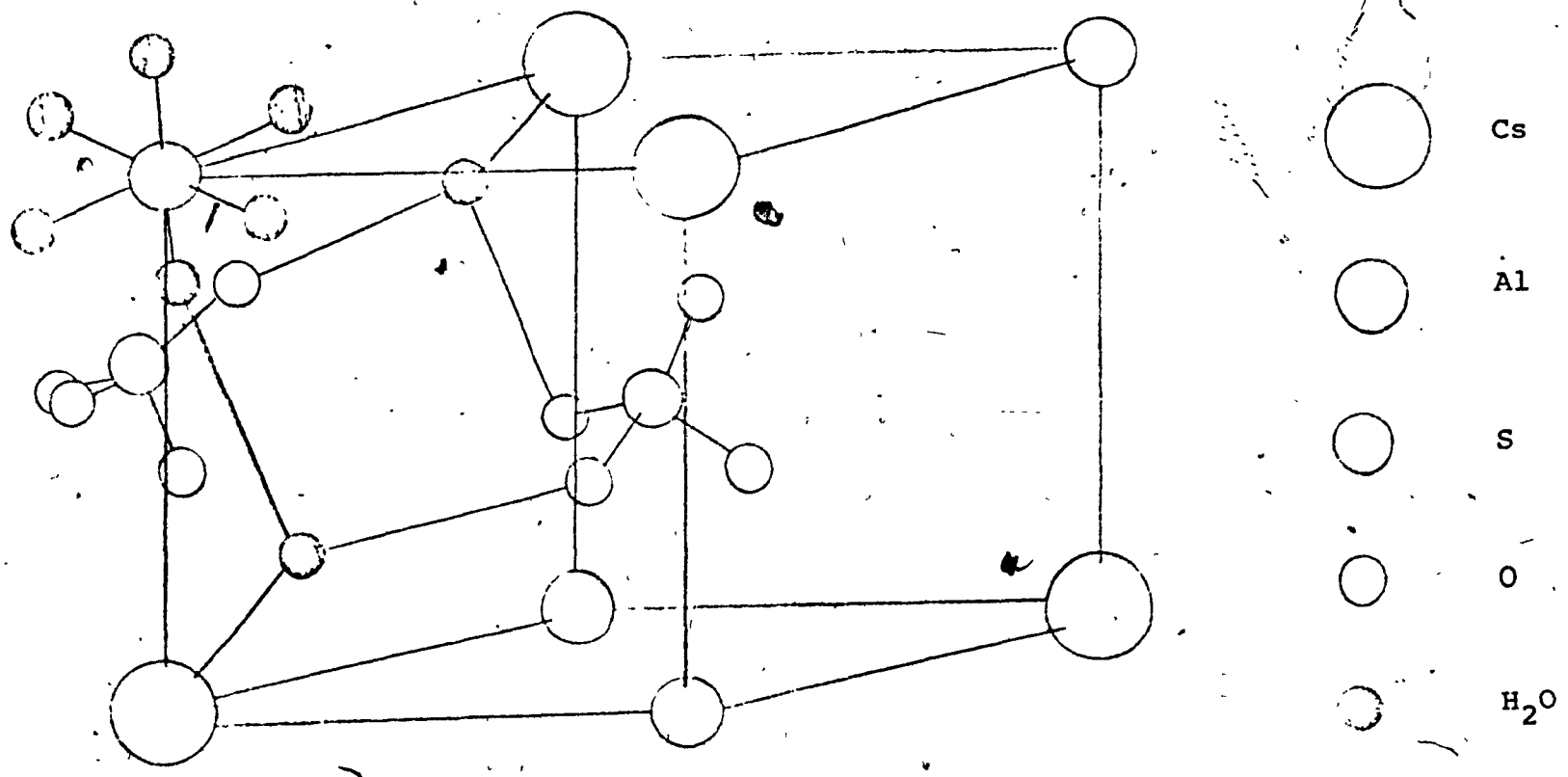

Figure 5. Crystal Structure of $CsAl(SO_4)_2 \cdot 12H_2O$

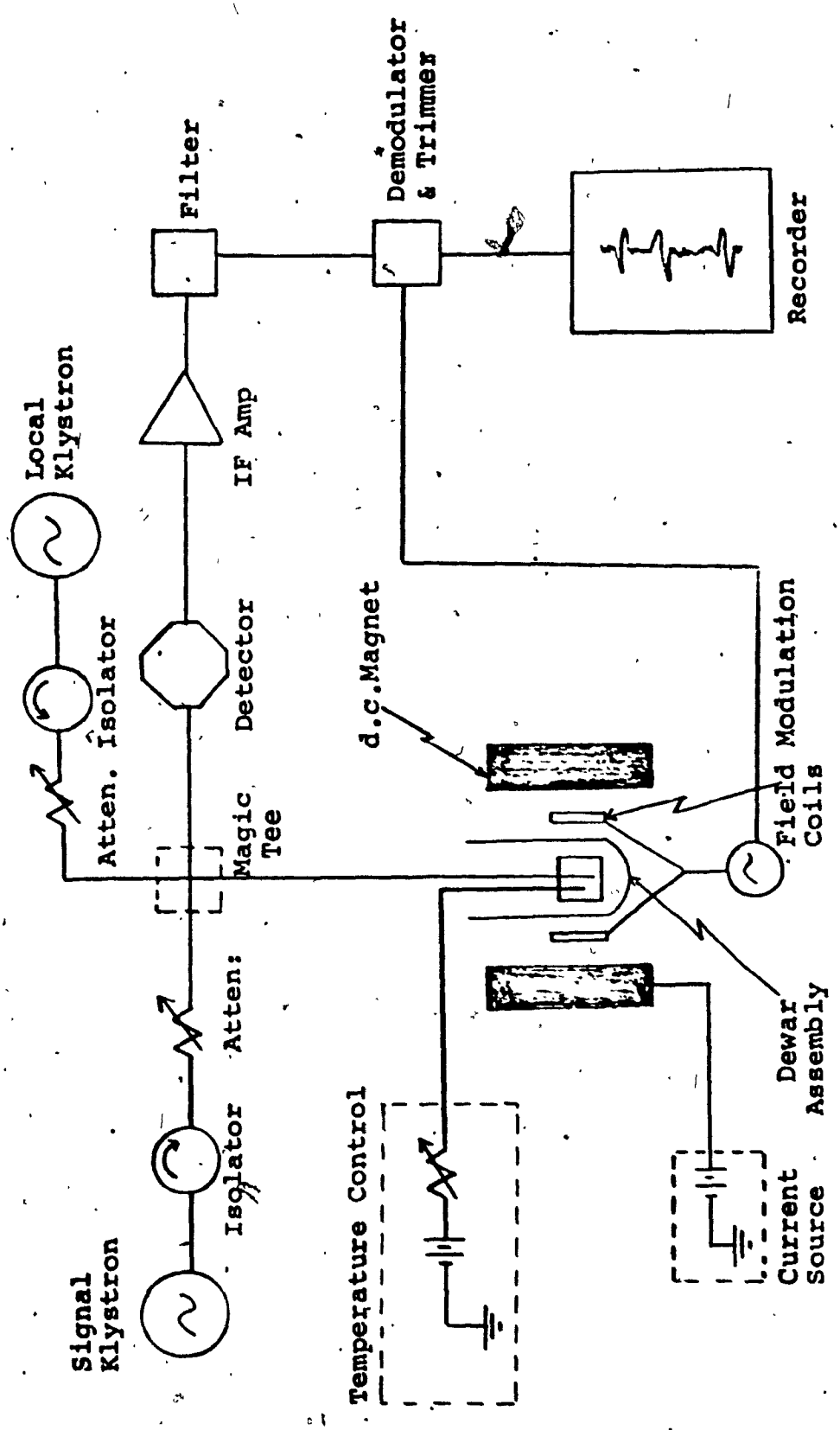

Figure 6. Schematic of EPR Spectrometer

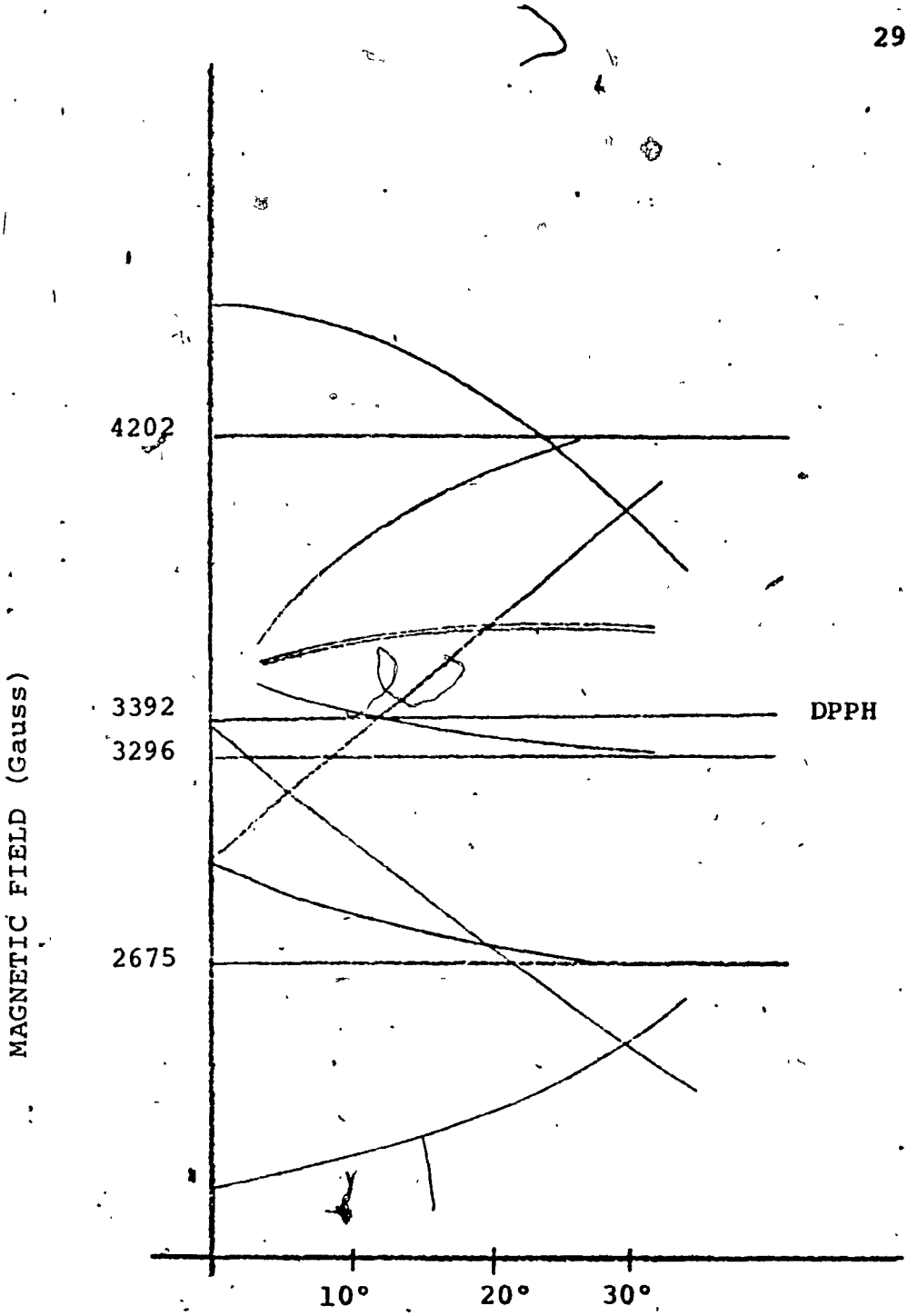

Figure 7. EPR Spectrum of Cr^{3+} in $CsAl(SO_4)_2 \cdot 12H_2O$ in the {111} plane at 4.2 °K.

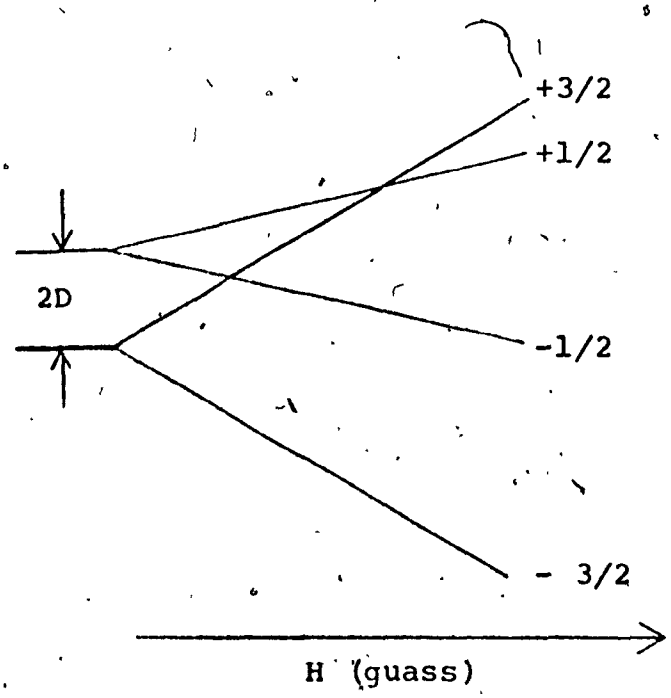

Figure 8. Energy level diagram of a S = 3/2 system and the magnetic field parallel to the crystalline field axis.

Figure 9

Calibration of Platinum Resistance Thermometer (Rosemount Engineering #137AA)

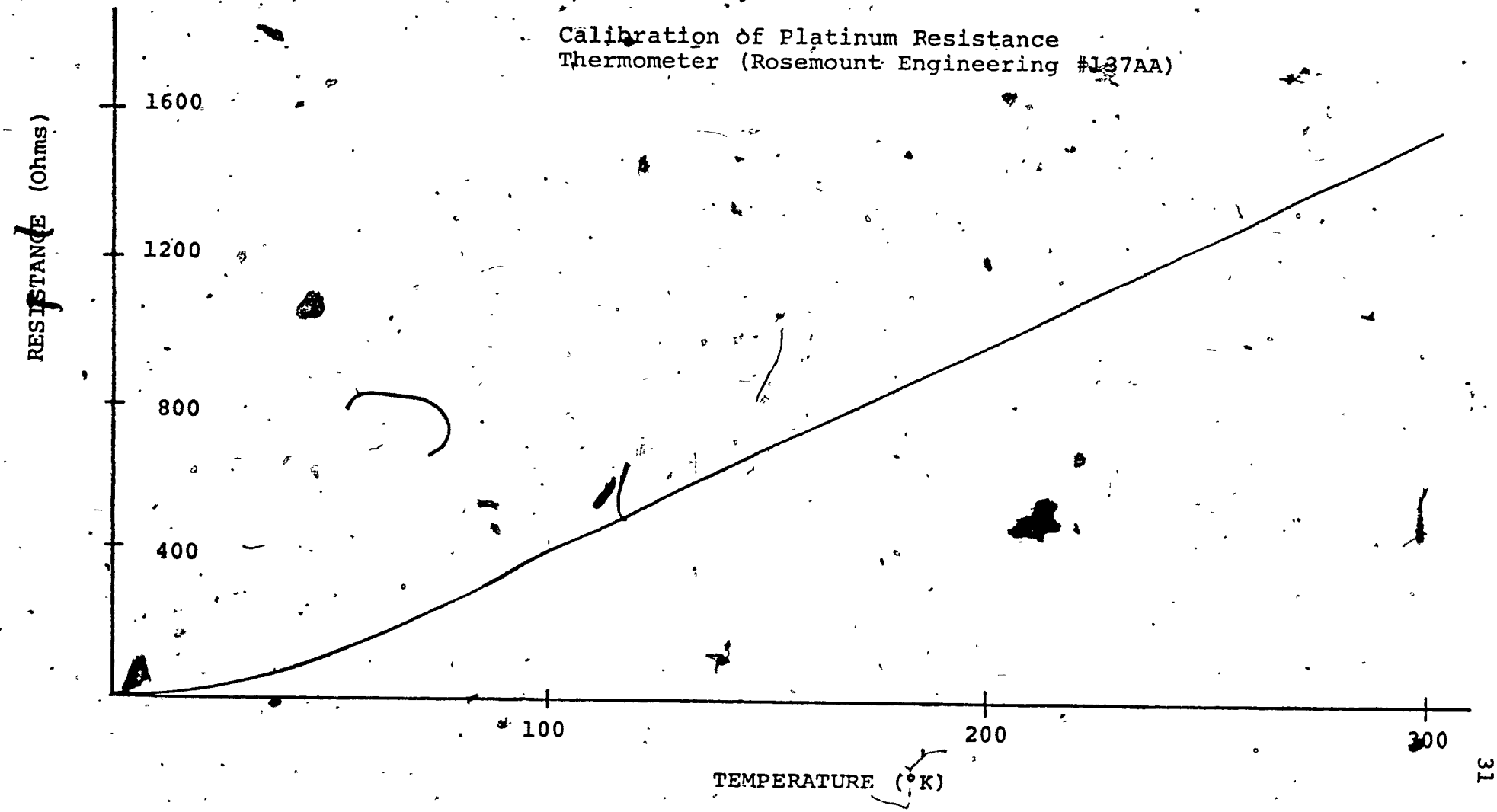

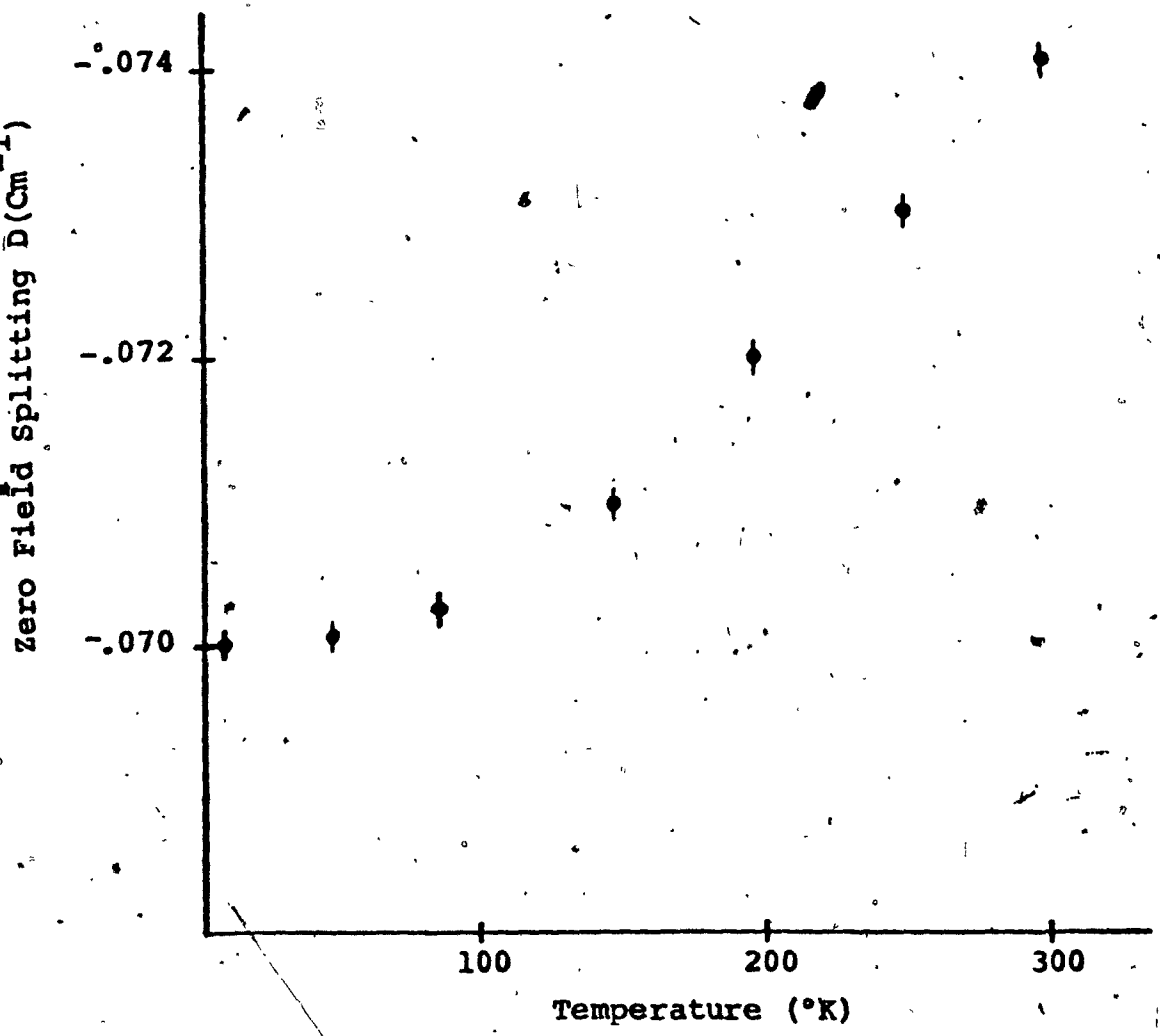

Figure 10. Variation of the zero field splitting parameter for Cr^{3+} in $CsAl(SO_4)_2 \cdot 12H_2O$ as a function of temperature.

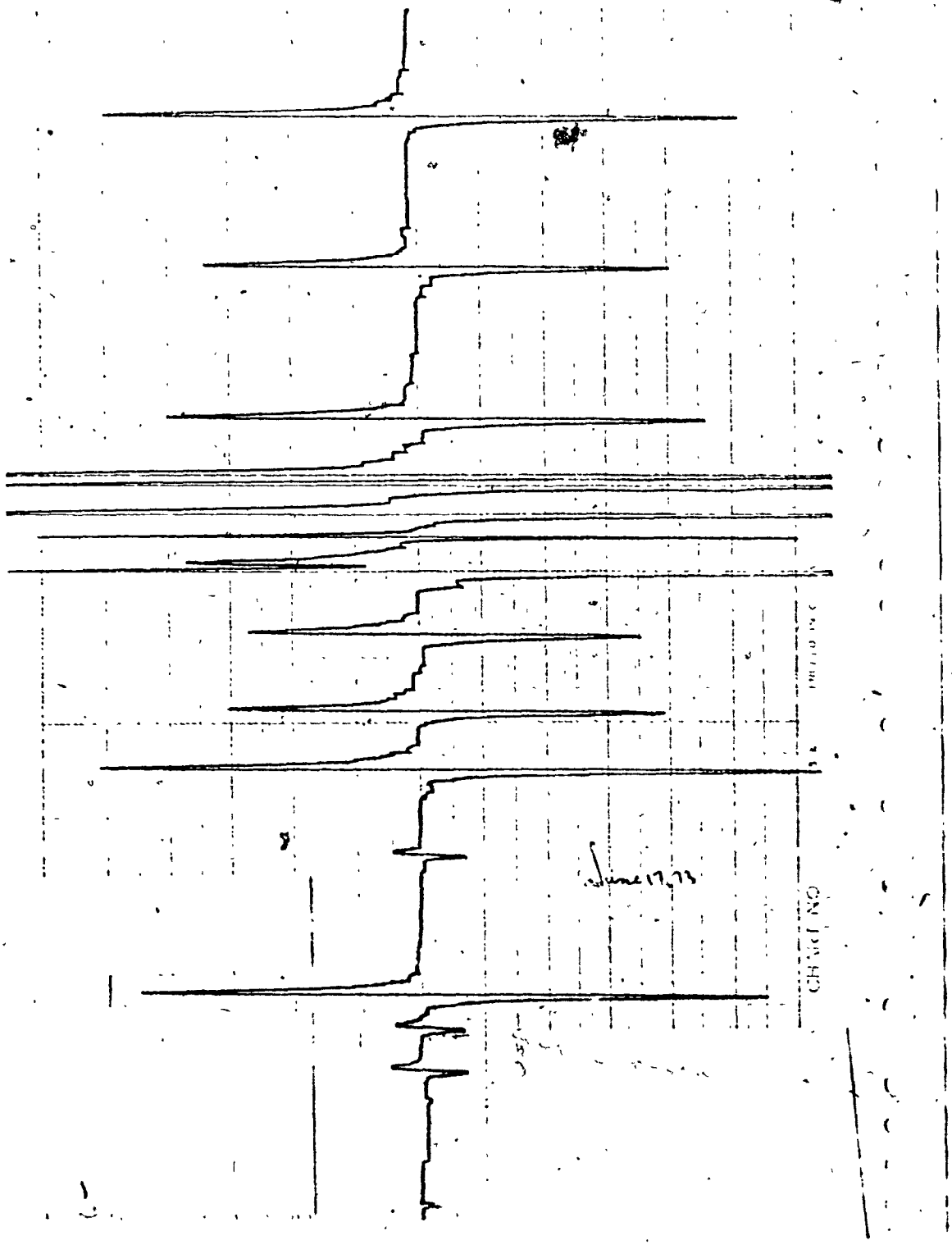

figure 11. ESR Chart recording of $CsAl(SO_4)_2.12H_2O$ doped with Cr^{3+}